

Hydrodynamic Similarity in an Oscillating-Body Viscometer¹

R. F. Berg²

Hydrodynamic similarity can be used to calibrate simply and accurately an oscillating-body viscometer of arbitrarily complicated geometry. Usually, an explicit hydrodynamic model based on a simple geometry is required to deduce viscosity from the transfer function of an oscillating body such as a vibrating wire or a quartz torsion crystal. However, at low Reynolds numbers the transfer function of any immersed oscillator depends on the fluid's viscosity only through the viscous penetration depth $\delta \equiv (2\eta/\rho\omega)^{1/2}$. (Here η and ρ are the fluid's viscosity and density and $\omega/2\pi$ is the oscillator's frequency.) This hydrodynamic similarity can be exploited if the oscillator is overdamped and thus is sensitive to viscosity in a broad frequency range. Even an oscillator of poorly known geometry can be characterized over a range of penetration depths by measurements in a fluid of known η and ρ over the corresponding range of frequencies. The viscosity of another fluid can then be compared to that of the calibrating fluid with high accuracy by varying the frequency so that the penetration depth falls within the characterized range. In the present work, hydrodynamic similarity was demonstrated with a highly damped viscometer comprised of an oscillating screen immersed in carbon dioxide. The fluid's density was varied between 2 and 295 kg · m⁻³ and the fluid's temperature was varied between 25 and 60°C. The corresponding variation of the viscosity was 50%.

KEY WORDS: calibration; hydrodynamic similarity; oscillating-body viscometer.

1. INTRODUCTION

The measurements reported here were motivated by the need to calibrate a viscometer intended to measure the viscosity of xenon near its critical

¹ Paper presented at the Twelfth Symposium on Thermophysical Properties, June 19–24, 1994, Boulder, Colorado, U.S.A.

² Thermophysics Division, Chemical Science and Technology Laboratory, National Institute of Standards and Technology, Gaithersburg, Maryland 20899, U.S.A.

point on board the Space Shuttle [1]. The viscometer was intentionally overdamped to make it insensitive to the Shuttle's vibrations. The geometry selected to achieve overdamping was too complicated to model accurately. Thus, further calibration was needed.

The calibration was achieved by exploiting a hydrodynamic similarity applicable to the hydrodynamics of any oscillating-body viscometer, provided the oscillations are small and the viscometer is sensitive to viscosity over a wide frequency bandwidth. Although hydrodynamic similarity most often refers to scaling of the Navier–Stokes equation with the Reynolds number, here the emphasis is on another similarity that exists for low-amplitude oscillatory flow. This method does not rely on a specific hydrodynamic model, and a single measurement with a fluid of known viscosity and density calibrates the viscometer for other fluids without knowledge of the viscometer's geometry.

The viscometer was an electrostatically driven screen. In tests, it was immersed in CO_2 at various densities and temperatures. The measurements of viscosity changes were consistent with the best viscosity measurements available in the literature. For example, at a density of $1.79 \text{ kg} \cdot \text{m}^{-3}$, when the viscosity was changed by 11%, the associated change in the oscillator's transfer function was correlated to within 0.2% by the use of hydrodynamic similarity. The remarkable consistency achieved in a wide range of conditions supports the validity of using hydrodynamic similarity as a calibration technique.

The present approach contrasts with the usual method relying on the hydrodynamic theory for an idealized geometry. For example, the model for a vibrating-wire viscometer begins with an infinite circular cylinder [2]. Corrections for nonideal features such as edges or ellipticity are almost always required, and they are either calculated from a hydrodynamic model or measured in ancillary experiments. These corrections must be known throughout the operating ranges of frequency, density, and viscosity.

2. HYDRODYNAMIC SIMILARITY

To understand the similarity concept demonstrated here, it is helpful to consider a linear harmonic oscillator with mass m , spring constant k , and dissipation coefficient $\nu(\omega)$. For an applied sinusoidal force $F(\omega)$ the displacement $x(\omega)$ is given by the transfer function

$$H(\omega) \equiv \frac{x(\omega)}{F(\omega)} = [-m\omega^2 + i\omega\nu + k]^{-1} \quad (1)$$

By measuring $H(\omega)$ of the immersed oscillator, one can infer the viscosity through its effect on the dissipation coefficient ν . It is useful to define the dimensionless quantities

$$\Omega \equiv \frac{\omega}{\omega_0} \quad \text{and} \quad Q \equiv \frac{m\omega_0}{\nu} \quad (2)$$

where $\omega_0 = (k/m)^{1/2}$ is the oscillator's resonance frequency in vacuum. In general, Q is a function of frequency. Equation (1) then becomes

$$k_{tr}H(\omega) = \frac{k_{tr}}{k} \left[(1 - \Omega^2) + \frac{i\Omega}{Q} \right]^{-1} \quad (3)$$

where the constant k_{tr} accounts for the (possibly unknown) transducer constants.

The linearized Navier-Stokes equation can be written in terms of a dimensionless velocity, pressure, time, and spatial derivative, u' , p' , t' , and ∇' by rescaling their dimensional equivalents with respect to a characteristic length R , a characteristic time ω^{-1} , and a characteristic pressure $\eta\omega$. The result,

$$\frac{\partial u'}{\partial t'} = \frac{\eta}{\rho\omega R^2} \nabla' p' + \frac{\eta}{\rho\omega R^2} \nabla'^2 u' \quad (4)$$

is an equation parameterized only by the ratio (R/δ) , where ρ and η are the fluid's density and viscosity, and δ is the viscous penetration length defined by

$$\delta \equiv \left[\frac{2\eta}{\rho\omega} \right]^{1/2} \quad (5)$$

The viscous dissipation term in Equation (3) can be similarly scaled by writing

$$\frac{i\Omega}{Q} = i\Omega \frac{(\nu' \eta R)}{(K \rho_s R^3)(\omega/\Omega)} = i\Omega^2 \left(\frac{\nu'}{2K} \right) \left(\frac{\rho}{\rho_s} \right) \left(\frac{\delta}{R} \right)^2 \quad (6)$$

where ρ_s is the density of the oscillator body and K is a constant geometric factor. The dimensionless dissipation coefficient ν' depends on geometry only through the ratio (R/δ) . By substituting Eq. (6) into Eq. (3), the transfer function can be written in terms of a function $B(R/\delta)$ characteristic of the viscometer's geometry, namely,

$$k_{tr}H(\omega) = \frac{k_{tr}}{k} \left[(1 - \Omega^2) + i\Omega^2 \left(\frac{\rho}{\rho_s} \right) B(R/\delta) \right]^{-1} \quad (7)$$

The most important feature of Eq. (7) is that *the oscillator's transfer function depends on the fluid's viscosity only through the viscous penetration length.*

Equation (7) is of limited use for a typical vibrating viscometer, which has $Q \gg 1$ and is sensitive to the fluid's viscosity only near $\Omega = 1$. In contrast, for a low- Q , or overdamped, oscillator, viscosity can be measured over a broad frequency range. Equivalently, at a fixed ρ and η , the viscometer is sensitive over a broad range of δ . In this case, the function $B(R/\delta)$ can be measured directly.

Equation (7) requires that the oscillator be characterized by only the undamped resonance frequency ω_0 , the factor k_{tr}/k , and the function $(\rho/\rho_s) B(\rho/\delta)$. The frequency ω_0 can be accurately measured in vacuum, and the ratio k_{tr}/k can be obtained directly by measuring the transfer function $H(\omega)$ in the limit of 0 Hz. The function $B(R/\delta)$ can be inferred from measurements of the oscillator's transfer function

$$B(R/\delta) = \frac{[(k/k_{tr}) H(\omega)]^{-1} - (1 - \Omega^2)}{i\Omega^2(\rho/\rho_s)} \quad (8)$$

The parameters ρ_s and R can be arbitrarily chosen because they can be absorbed into the function $(\rho/\rho_s) B(R/\delta)$.

Even if the oscillator's geometry is accurately known, incomplete knowledge of its hydrodynamics can require measurement of B . For example, measurement of an edge correction with a calibrating fluid is required for oscillating-disk viscometers [2]. For high- Q oscillators, this is accomplished by operation at one frequency with calibrating fluids of various kinematic viscosities. This strategy is limited by the accuracy of the calibrating fluids' viscosities.

In contrast, a low- Q oscillator can be calibrated by measurements at multiple frequencies in a single fluid. Furthermore, if the viscometer is used only to measure viscosity changes relative to a reference state of the fluid, this second strategy can give a high accuracy without the use of a calibrating fluid.

3. APPARATUS

The viscometer's oscillating body consisted of a 7×19 -mm rectangle of nickel screen. (See the inset to Fig. 2) The screen's wires were not circular in cross section, and their greatest thickness was 0.03 mm in the plane of the screen. They were spaced every $847 \mu\text{m}$ on a square grid. The screen was suspended from a yoke by two of its wires which extended outward to form a pair of torsion wires. Four parallel electrodes applied electrostatic forces to oscillate the screen about its torsion axis. The electrodes also

formed a capacitance bridge that was used to detect the displacement of the screen. Typically the amplitude of motion at the ends of the screen was $10\ \mu\text{m}$.

The viscometer was contained in a cylindrical copper cell with an internal volume of $11.19 \pm 0.02\ \text{cm}^3$. A small valve attached to a fill line near the cell allowed the cell to be filled, detached from the gas manifold, weighed, and then placed in a thermostat.

The drive force was proportional to a swept sine voltage, and the capacitance bridge's output voltage was a linear function of the displacement. The drive and detected voltages were recorded in a commercial spectrum analyzer, which then calculated the associated transfer function $H(\omega)$. The thermostat, cell, viscometer, and measurement technique are described in more detail elsewhere [1].

4. MEASUREMENTS

4.1. Choice of Fluid

Carbon dioxide was chosen as the test fluid because accurate viscosity data for CO_2 are available at moderate temperatures and pressures at kinematic viscosities comparable to that of xenon at its critical density (see Table I). These criteria excluded liquids such as water and toluene and gases such as argon and nitrogen.

For calibration I used previous viscosity measurements included in the recent correlation of Vesovic et al. [3]. Four density ranges were considered: "low" (where $\partial\eta/\partial\rho$ is small), "moderate" but below the critical region, the critical region, and above the critical region. The most accurate measurements were made at low densities near room temperature. For these data the representation of Kestin et al. [4] was used. Within 0.2%, the data from Kestin's group agree with both the more recent measurements by Vogel and Barkow [5] and the correlation of Ref. 3 over the 25–61°C temperature range used in the present measurements.

Table I. Approximate Kinematic Viscosity ($\text{m}^2 \cdot \text{s}^{-1}$) for Representative Densities of CO_2 Near Room Temperature^a

Fluid	CO_2 (3)	CO_2 (30)	CO_2 (300)	Xe (ρ_c)
η/ρ	5.1×10^{-6}	5.1×10^{-7}	7.6×10^{-8}	4.7×10^{-8}

^a The number in parentheses is the density in $\text{kg} \cdot \text{m}^{-3}$. Also shown is the minimum value for xenon.

At moderate densities, the correlation of Kestin et al. [6], who reported viscosity measurements made at 31.6°C and at densities up to 307 kg · m⁻³, was used. At the higher densities, their values disagree by as much as 1% with the older measurements of Kestin et al. [7]. This latter set was useful because it reported the temperature dependence at moderate densities.

No measurements were made at densities near or above the critical density of CO₂.

4.2. Technique

The present tests were made to demonstrate the applicability of hydrodynamic similarity for the present oscillating viscometer. The demonstration could have failed for various reasons. For example, the flow could have been too large for the linearized Navier–Stokes equation to apply, there could have been coupling to a bending mode of the screen, or the transducers could have had an unexpected frequency dependence. To look for such effects, a wide range of conditions were covered. The samples spanned a factor of 165 in density, corresponding to a 50% change in the viscosity, and measurements were made in the temperature range from 25 to 61°C.

The oscillator's transfer function was measured over the range 0.03 to 25 Hz at the five densities and temperatures listed in Table II. The densities, determined by weighing the filled cell, were chosen to fall near those used by Kestin et al. [7]. (The lowest density was achieved by filling the

Table II. Viscosity Values (10⁻⁵ Pa · s) Used in the Calibration Tests^a

T (°C)	ρ (kg · m ⁻³)				
	1.79	18.9	90.1	242.8	295.1
25.6	1.495 [4]				
31.6		1.530 [6]	1.616 [6]	2.054 [6]	2.270 [6]
31.6				2.028 [7]	
34.6				2.046 [7]	
40.6	1.568 [4]			2.086 [7]	
60.6	1.663 [4]				

^a Data sources are indicated by reference numbers in brackets. Although the densities and temperatures were chosen to be close to those used in the referenced studies, small interpolations in density and temperature were necessary.

cell at ambient temperature and pressure.) Measurements were also made at frequencies down to 0.001 Hz to obtain the coefficient k_{tr}/k . Preceding these tests, the oscillator's resonance frequency and Q were measured in vacuum between 7 and 81°C.

5. RESULTS

5.1. Density Dependence Near Room Temperature

Figure 1 shows the transfer function measured at four of the five densities. (The data at $242.8 \text{ kg} \cdot \text{m}^{-3}$ are omitted for clarity.) The viscometer was sensitive to viscosity changes over most of the measured frequency range. For example, at 8 Hz, a viscosity change of 10% would change the oscillator's amplitude by about 8%.

Values of the function $B(R/\delta)$ were derived from Eq. (8). The results, which include small corrections for the spring's anelastic character and the effects of four low-pass electronic filters [1], are shown in Fig. 2. Also plotted is the value of $B(R/\delta)$ calculated for a transversely oscillating cylinder [10] of radius $R \equiv 13.8 \mu\text{m}$. The strongest deviations from the cylinder model occur at large viscous penetration lengths. This is to be expected for $R/\delta < 0.033$, where δ is half the distance between screen wires.

Three adjustments were made to the data. First, the noisier data below 1 Hz were dropped. Second, data above 10 Hz were dropped because the

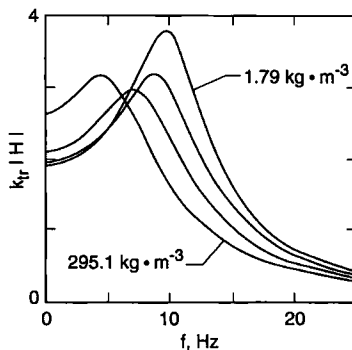


Fig. 1. The magnitude of the transfer function $H(\omega)$ measured in CO_2 at 1.79, 18.9, 90.1, and $295.1 \text{ kg} \cdot \text{m}^{-3}$. The lowest-density data were obtained at 25.6°C, and the remainder were acquired at 31.6°C.

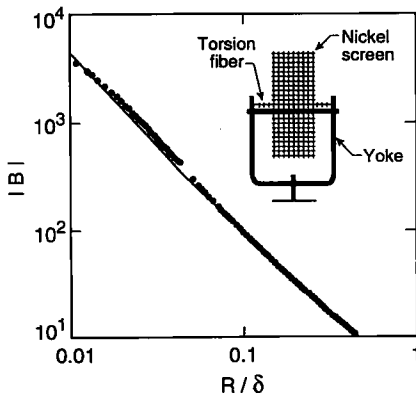


Fig. 2. The magnitude of the function $B(R/\delta)$ derived from the transfer function data shown in Fig. 1. The reference length is $R \equiv 13.8 \mu\text{m}$, and the viscosity values are from Kestin et al. [6]. The curve was calculated from the model of an infinite transversely oscillating cylinder. The inset shows the oscillating screen.

effects of the torsion fiber's anelasticity and of the electronic filters were not accurately modeled at higher frequencies. Third, the value of the viscosity used at $295.1 \text{ kg} \cdot \text{m}^{-3}$ from Kestin et al. [6] was lowered by 1%. The size of the third adjustment was chosen to match the value of $B(R/\delta)$ derived at $295.1 \text{ kg} \cdot \text{m}^{-3}$ with that derived at lower densities, and it is justified in two ways. First, it yields a curve with continuous slope as well as value. Second, the amplitude of the adjustment is consistent both with the scatter of the original data and with the disagreement between Ref. 6 and Ref. 7: Near $300 \text{ kg} \cdot \text{m}^{-3}$ the viscosity values of Ref. 7 are about 1% less than those of Ref. 6.

After these adjustments, the data were fully consistent with the expected hydrodynamic similarity. To within experimental uncertainty, both the magnitude and the phase of the transfer function defined smooth, density-independent curves spanning a factor of 40 in δ .

5.2. Temperature Dependence at Moderate Density

Measurements of $H(\omega)$ were obtained at 31.6, 34.6, and 40.6°C at a constant density of $242.8 \text{ kg} \cdot \text{m}^{-3}$. For consistency in this comparison, only

data from one investigation, that of Kestin et al. [7], were used. Over the range $0.2 < R/\delta < 0.3$ the data for $|B/B_c|$ obtained at 31.6 and 40.6°C were consistent to within 0.1% of the viscosity. The viscosity changes by 2.9% between these two temperatures. Although noisier, the data at 34.6°C are higher than those at 31.6 and 40.6°C, corresponding to a viscosity disagreement of -0.2%. The source of this tiny disagreement is not known.

5.3. Temperature Dependence at Low Density

The oscillator's transfer function $H(\omega)$ was measured at 25.6, 40.6, and 60.6°C at a nearly constant density of $1.79 \text{ kg} \cdot \text{m}^{-3}$. The temperature uncertainty was 0.1 K. Although the 11% variation in the viscosity was less than that resulting from varying the density, these tests are important because the most accurate data for the viscosity are at low density.

The consistency of the data at low density can be seen in Fig. 3, which uses 25.6°C as a reference state and compares the viscosity at 40.6 and 60.6°C to the values from Ref. 4. Although the deviations are greater than the stated accuracy of Kestin et al. [4], they are consistent with the correlation of Ref. 3. Thus, the use of hydrodynamic similarity was consistent with the most accurate viscosity data available.

These comparisons at low density did not measure absolute viscosity; however, they did test the viscometer's ability to measure accurately

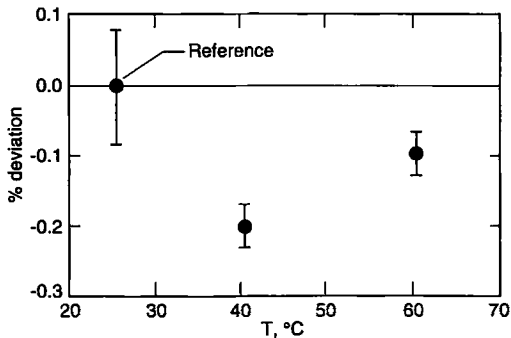


Fig. 3. Data at the lowest density are compared by averaging the values of $|B(R/\delta)|$ in the range $0.020 < R/\delta < 0.025$ and then calculating the corresponding variations in viscosity. The bars show $\pm 1\sigma$ scatter in the data. At the reference state of 25.6°C, the viscosity is defined to be equal to that found by Kestin et al. [4]. This point and the deviations at 40.6 and 60.6°C from the values of Ref. 4 fall within a range of $\pm 0.2\%$.

the variation of viscosity with temperature. The agreement in the latter quantity is

$$\frac{\Delta\eta}{\eta(60.6^{\circ}\text{C}) - \eta(25.6^{\circ}\text{C})} = \frac{0.2\%}{11\%} = 2\% \quad (9)$$

where $\Delta\eta$ is the standard uncertainty (i.e., estimated standard deviation) in the viscosity.

ACKNOWLEDGMENTS

Michael Moldover provided essential support and detailed comments. This work was supported in part under NASA Contract C32014-C.

REFERENCES

1. R. F. Berg and M. R. Moldover, Science Requirements Document, report to NASA Lewis Research Center (1994).
2. A. Nagashima, J. V. Sengers, and W. A. Wakeham, *Measurement of the Transport Properties of Fluids* (Blackwell Scientific, Melbourne, FL, 1991).
3. V. Vesovic, W. A. Wakeham, G. A. Olchowy, J. V. Sengers, J. T. R. Watson, and J. Millat, *J. Phys. Chem. Ref. Data* **19**:763 (1990).
4. J. Kestin, S. T. Ro, and W. A. Wakeham, *J. Chem. Phys.* **56**:4114 (1972).
5. E. Vogel and L. Barkow, *Z. Phys. Chem. Leipzig* **267**:1038 (1986).
6. J. Kestin, Ö. Korfali, and J. V. Sengers, *Physica* **100A**:335 (1980).
7. J. Kestin, W. H. Whitelaw, and T. F. Zien, *Physica* **30**:161 (1964).
8. H. Iwasaki and M. Takahashi, *J. Chem. Phys.* **74**:1930 (1981).
9. R. F. Berg and M. R. Moldover, *J. Chem. Phys.* **93**:1926 (1990).
10. G. G. Stokes, *Mathematical and Physical Papers, Vol. III* (Cambridge University, London, 1922), p. 11; R. G. Hussey and P. Vujacic, *Phys. Fluids* **10**:96 (1967); R. E. Williams and R. G. Hussey, *Phys. Fluids* **15**:2083 (1972).